HemaSphere

EHA EUROPEAN HEMATOLOGY ASSOCIATION

Article
Open Access

In Humanized Sickle Cell Mice, Imatinib Protects Against Sickle Cell–Related Injury

Enrica Federti[1], Alessandro Matte[1], Antonio Recchiuti[2], Francesca Garello[3], Alessandra Ghigo[3], Wassim El Nemer[4], Enzo Terreno[3], Angela Amoresano[5], Domenico Mattoscio[2], Franco Turrini[6], Christophe Lebouef[7,8,9], Anne Janin[7,8,9], Antonella Pantaleo[10], Roberta Russo[11], Mickael Marin[4], Iana Iatcencko[1], Veronica Riccardi[1], Angela Siciliano[1], Achille Iolascon[11], Carlo Brugnara[12], Lucia De Franceschi[1]

GRAPHICAL ABSTRACT

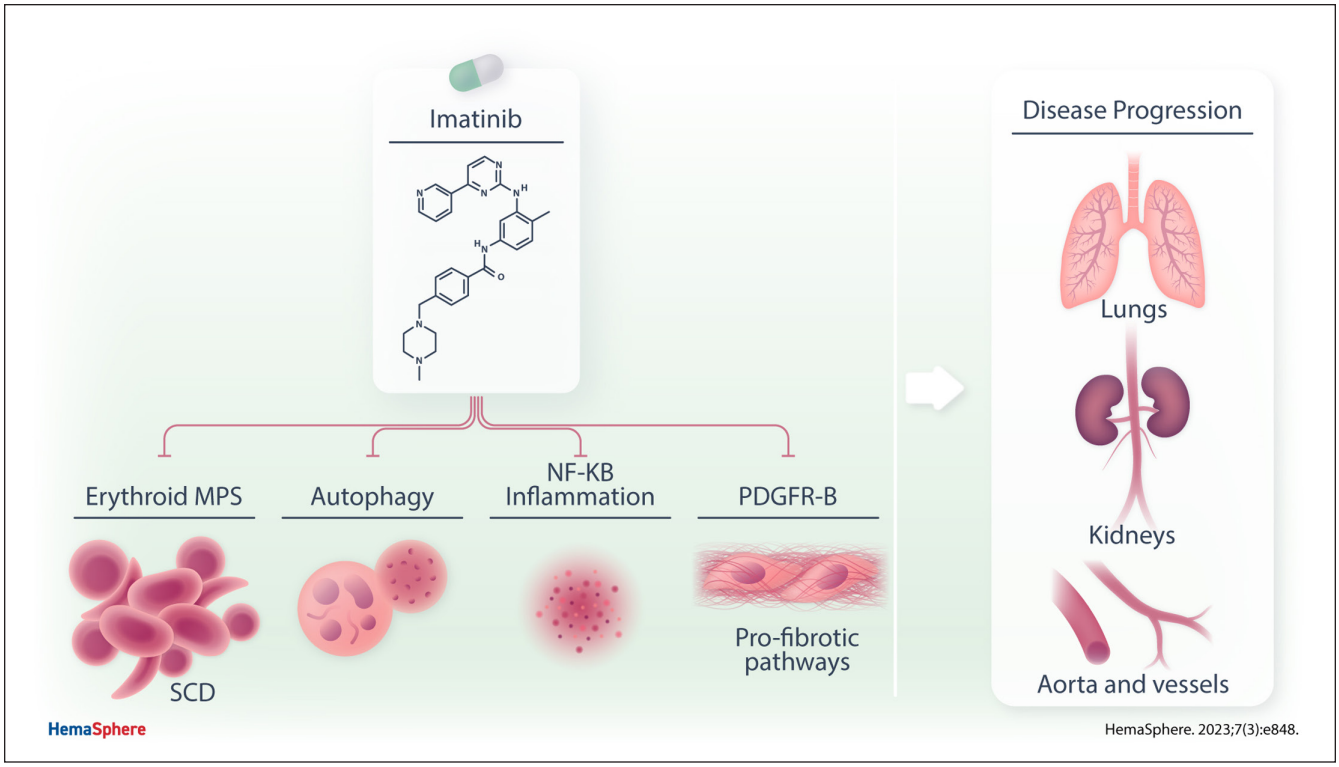

HemaSphere

EHA EUROPEAN HEMATOLOGY ASSOCIATION

Article
Open Access

In Humanized Sickle Cell Mice, Imatinib Protects Against Sickle Cell–Related Injury

Enrica Federti[1], Alessandro Matte[1], Antonio Recchiuti[2], Francesca Garello[3], Alessandra Ghigo[3], Wassim El Nemer[4], Enzo Terreno[3], Angela Amoresano[5], Domenico Mattoscio[2], Franco Turrini[6], Christophe Lebouef[7,8,9], Anne Janin[7,8,9], Antonella Pantaleo[10], Roberta Russo[11], Mickael Marin[4], Iana Iatcencko[1], Veronica Riccardi[1], Angela Siciliano[1], Achille Iolascon[11], Carlo Brugnara[12], Lucia De Franceschi[1]

Correspondence: Lucia De Franceschi (lucia.defranceschi@univr.it).

ABSTRACT

Drug repurposing is a valuable strategy for rare diseases. Sickle cell disease (SCD) is a rare hereditary hemolytic anemia accompanied by acute and chronic painful episodes, most often in the context of vaso-occlusive crisis (VOC). Although progress in the knowledge of pathophysiology of SCD have allowed the development of new therapeutic options, a large fraction of patients still exhibits unmet therapeutic needs, with persistence of VOCs and chronic disease progression. Here, we show that imatinib, an oral tyrosine kinase inhibitor developed for the treatment of chronic myelogenous leukemia, acts as multimodal therapy targeting signal transduction pathways involved in the pathogenesis of both anemia and inflammatory vasculopathy of humanized murine model for SCD. In addition, imatinib inhibits the platelet-derived growth factor-B–dependent pathway, interfering with the profibrotic response to hypoxia/reperfusion injury, used to mimic acute VOCs. Our data indicate that imatinib might be considered as possible new therapeutic tool for chronic treatment of SCD.

INTRODUCTION

In rare diseases, drug repurposing, which explores known and unexpected effects of molecules already in clinical use for treatment of other disorders is a valuable strategy.[1–3] Different approaches might be put in place to select candidate molecules to be re-purposed. Among them, an experimental data-driven strategy might be extremely interesting in the context of rare diseases.[1–3]

Sickle cell disease (SCD) is a genetically determined rare hemolytic anemia characterized by the presence of the pathologic hemoglobin S (HbS), which polymerizes under low oxygen conditions.[4–9] HbS polymerization leads to generation of rigid and dense erythrocytes with reduced survival in the circulation, resulting in chronic hemolysis and anemia.[9,10]

SCD is also characterized by acute and chronic painful episodes, most often in the context of vaso-occlusive crisis (VOC), a definition based on the notion that occlusion of small vessels and/or capillaries by sickled cells is the triggering mechanism for the generation of inflammation and pain. In addition to red cells, neutrophils, inflammatory-activated vascular endothelial cells, cytokines, and proadhesive molecules such as selectins or vascular cell adhesion molecule-1 (VCAM-1), have been identified to contribute to the pathogenesis of VOCs.[4–9] The impairment of proresolving mechanisms reported in humanized SCD mice further sustains vascular vulnerability and dysfunction.[10]

Progress in the knowledge of pathophysiology of SCD has allowed the development of new therapeutic options such as oral antisickling agent (Voxelotor),[11,12] and injectable monoclonal antibody against P-selectin (Crizalinzumab), which are currently in clinical use.[13] However, the persistence of VOCs, as well as chronic disease progression, still represent unmet therapeutic needs, which require additional therapeutic approaches. We recently reported that imatinib, an oral tyrosine kinase inhibitor developed for the treatment of chronic myelogenous leukemia (CML), reduced the release of free hemoglobin and erythroid vesiculation of sickle red cells in vitro, and affected

[1]Department of Medicine, University of Verona & AOUI Verona, Policlinico GB Rossi, Verona, Italy
[2]Department of Medical, Oral, and Center for Advanced Studies and Technology (CAST), University "G. d'Annunzio" Chieti-Pescara, Italy
[3]Department of Molecular Biotechnology and Health Sciences, Molecular Biotechnology Center, University of Torino, Italy
[4]Etablissement Français du Sang, UMR 7268 ADES, Faculte de Medicine Timone, Marseille, France
[5]Department of Chemical Sciences, University Federico II of Napoli, Italy
[6]Department of Oncology, University of Torino, Italy
[7]INSERM, U1165, Paris, France
[8]Université Paris 7 - Denis Diderot, Paris, France
[9]AP-HP, Hôpital Saint-Louis, Paris, France
[10]University of Sassari, Italy
[11]Dipartimento di Medicina Molecolare e Biotecnologie Mediche, Università degli Studi di Napoli Federico II, and CEINGE Biotecnologie Avanzate, Naples, Italy
[12]Department of Laboratory Medicine, Boston Children's Hospital, Harvard Medical School, Boston, MA, USA
Supplemental digital content is available for this article.

HemaSphere (2023) 7:3(e848).
http://dx.doi.org/10.1097/HS9.0000000000000848.
Received: November 3, 2022 / Accepted: January 19, 2023

ex vivo sickle red cell adhesion to activated vascular endothelial cells.[1] Case reports have described uncontrolled improvements in severity and recurrence of VOCs in SCD patients treated with imatinib due to concomitant CML.[14–16] In addition, improvement of pain perception, blood brain permeability as well as neuroinflammation has been previously reported in a mouse model for SCD (Hemoglobin SS-Berkley mice) treated with imatinib.[17–19] Imatinib displays protective effects in murine models of acute lung injury or kidney disease related to diabetes,[20–25] preventing the inflammatory-mediated activation of nuclear factor kappa-B (NF-kB) and modulating the function of the receptor for platelet-derived growth factor-B (PDGFR-B) and fibroblast growth factor receptor (FGF-R), which are involved in intravascular matrix remodeling and profibrotic events.[20–27]

In this study, using a humanized mouse model for SCD, we focused on acute, hypoxia-mediated sickle cell–related organ damage. We report that imatinib protects against hypoxia/reoxygenation (H/R)–induced lung and kidney damage. By combining complementary approaches such as in vivo visualization of VCAM-1 expression by magnetic resonance imaging (MRI) and immunoblot analysis with specific antibody against VCAM-1, we find that imatinib beneficially affects inflammatory vasculopathy. We also find a reduction in profibrotic pathways involving PDGFR-B/FGF-R signaling and miRNA such as let-7c or miR-200a in both lung and kidney of SCD mice treated with imatinib. Collectively, our data indicate that imatinib modulates signal transduction pathways in sickle red cells which ultimately downmodulate the inflammatory response related to H/R, limiting the severity of sickle cell–related organ damage. Thus, imatinib should be considered as a potential new therapeutic tool for patients affected by SCD.

MATERIALS AND METHODS

Mouse model and experimental design

Experiments were performed on 4–6-month-old sex matched healthy control ($Hba^{tm1(HBA)Tow}$ $Hbb^{tm3(HBG1,HBB)Tow}$) and SCD ($Hba^{tm1(HBA)Tow}$ $Hbb^{tm2(HBG1,HBB*)Tow}$) mice. The animal protocol was approved by the Animal Care and Use Committee of the University of Verona (CIRSAL). Whole blood was collected from each mouse under isoflurane anesthesia via retro-orbital venipuncture with heparinized microcapillaries. Hematological parameters and red cell indices were evaluated with a Sysmex XN-1000 Hematology Analyzer (Kobe, Japan).[28–31] Biochemical assays in heparinized plasma were performed using standard human biochemical assays, as previously reported.[10,32–35] Values of soluble cytokines and soluble adhesion molecules (Intracellular adhesion moecule 1 [ICAM-1], tumor necrosis factor-α [TNF-α], and E-Selectin) were determined by a Luminex Mouse Magnetic Assay (10-Plex) LXSAMSM-10 following the manufacturer instructions (R&D Systems, MI). The samples were analyzed using the Bio-Plex 200 System (Bio-Rad Laboratories, CA). Organs were immediately removed and divided into 2 portions which were either immediately frozen in liquid nitrogen or fixed in 10% formalin and embedded in paraffin for histology (see Suppl. Methods). Vehicle (tap water) or imatinib (50 mg/kg/d) were administrated by gavage for 3 weeks. The dosage of imatinib was based on previous pharmacokinetic studies in rodents, which yielded concentrations in plasma similar to those observed in patients.[36] Imatinib liver concentration in healthy (AA) and sickle (SS) mice treated with either vehicle or imatinib was determined by MRM (Suppl. Figure 1Sa). Bosutinib (150 mg/kg/d) was administrated by gavage for 11 days.[37] Among the new generation of tyrosine kinase inhibitors, we chose to test bosutinib, which shares some functional similarities with imatinib except for its effect on PDGF-R. No difference gender related was observed in either vehicle or imatinib/bosutinib-treated animals (eg, Suppl. Figure 13SA, central panel; Suppl. Figure 14SB, C, D). Details are reported in Suppl. Methods. As shown in Figure 1Sb, imatinib liver concentration was similar in healthy AA and SS mice treated with imatinib 50 mg/kg/d for 3 weeks.

When indicated, mice underwent a hypoxia/reoxygenation stress (H/R): 10 hours hypoxia (8% oxygen) followed by 3 hours reoxygenation (21% oxygen) to mimic acute VOC as previously described.[10,28] Details are reported in Suppl. Methods.

Lung, kidney, and liver histological analysis

Paraffin-embedded tissue blocks were cut into 2–3 μm sections and mounted on adhesion microscope glass slides for Hematoxylin-Eosin, PAS and Perls' staining for iron content. The analysis was performed on 4 different fields at a magnification 200×. Tissue pathological analysis, inflammatory cell infiltrate, the presence of thrombi and iron deposition were carried out by blinded pathologists as previously described.[10,28,38]

Molecular analyses and immunoblot analyses

See Suppl. Methods for details.[10,28,39]

Live imaging

Transthoracic echocardiography

Cardiac function was evaluated in mice anesthetized with 1% isoflurane using a Vevo 2100 High Resolution Imaging System (Visual Sonics Inc, Toronto, Canada) equipped with a 30-MHz probe (MS550D) (VisualSonics, Toronto, Canada). Echocardiographic parameters were measured under the long-axis M-mode when heart rate was about 450 bpm.[28,40]

Magnetic resonance imaging

MRI studies were performed on a Bruker Icon (1 T) under 1% isoflurane anesthesia. Vehicle or imatinib-treated mice were imaged before (PRE) and 24 hours after the intravenous administration of VCAM-1–targeted micelles (0.05 $mmol_{Gd}$/kg body weight).[41] Details are reported in Suppl. Methods.

Flow cytometric analysis of kidney inflammatory cell infiltrates

Right kidney was harvested and immediately processed for flow cytometric analysis. The following antibodies were used: anti CD45-V450, Ly6G APC-Cy7, B220 PE-Cy7, CD3 FITC, CD4 PE, CD8 PerCP-Cy5.5 (ThermoFisher Scientific, Waltham).[42,43] Details are reported in Suppl. Methods.

Statistical analysis

Normality was assessed with Shapiro-Wilk test. Two tailed unpaired Student t-test or 2-way analysis of variance with Tukey's multiple comparisons were used for data analyses. Data show values from individual mice and are presented with mean ± standard error of the mean. Differences with $P < 0.05$ were considered significant.

RESULTS

Imatinib improves anemia and reduces inflammation in SCD mice exposed to hypoxia/reoxygenation

Under normoxia conditions, imatinib significantly increased Hct (SS imatinib 36.5 ± 1.3% versus SS vehicle 30.9 ± 1.2%, n = 6 per group; $P < 0.05$) and hemoglobin values in SCD mice (SS imatinib 9.9 ± 0.6 g/dL versus Hb SS vehicle 8.6 ± 0.8 g/dL n = 6; $P < 0.05$). A reduction in reticulocyte count (SS imatinib 1.4 ± 0.2 cells × 10^6/μL versus SS vehicle 2.3 ± 0.14 cells × 10^6/μL, n = 6; $P < 0.05$) was also observed with no significant changes in neutrophil count (data not shown).

Imatinib-treated mice were then exposed to hypoxia/reoxygenation (H/R), a consolidated model to mimic acute sickle cell–related VOC.[10,28,44] Imatinib reduced H/R-induced hemolysis as supported by higher Hct, Hb, and lower lactate dehydrogenase and red cell distribution width values compared with

vehicle-treated SCD mice. This agrees with the reduction in liver Perls' staining in humanized SCD mice, a visual assessment of liver iron accumulation related to hemolysis[45] (Figure 1A, B and Suppl. Figure 1Sa, b). In SCD mice treated with imatinib and exposed to H/R, we found a reduction in the subset of erythrocytes exposing phosphatidylserine (assessed as Annexin-V positivity, Figure 1C).

We have previously reported that in vitro exposure of human sickle erythrocytes to imatinib reduces band 3 Tyrosine (Tyr-) phosphorylation and release of erythroid vesicles.[1] We found a significant reduction in both erythroid total Tyr-phosphorylation and band 3 Tyr-phosphorylation in SCD mice treated with imatinib and exposed to H/R when compared with vehicle-treated SCD animals (Suppl. Figure 2Sa). This was accompanied by a significant reduction in the release of erythroid microvesicles (Figure 1D, Suppl. Figure 2Sb).

Imatinib-treated SCD mice exposed to H/R exhibited lower values of CRP, a marker of systemic inflammation, as well as of circulating neutrophils (Figure 1E). Plasma TNF-alpha, an acute inflammatory phase cytokine, P-selectin and ICAM-1, markers of vascular endothelial activation, were also significantly decreased (Suppl. Figure 3Sc).

The adhesion of leukocyte from both healthy (AA) and SCD mice to a TNF-α activated vascular endothelial surface in a microfluidic chamber was also significantly reduced by the presence of imatinib (Suppl. Figure 4S).[10]

These data indicate that imatinib reduces H/R-induced hemolysis and positively modulates systemic inflammatory response, preventing neutrophils adhesion to inflammatory activated vascular endothelial cells.

Imatinib enhances sickle red cell and polymorphonuclear leukocytes efferocytosis by macrophages

We set out to determine whether efferocytosis of sickle red cells and neutrophils, a mechanism essential for removal of damaged cells and resolution of inflammation, could be modified by imatinib. In SCD mice, imatinib treatment significantly increased the percentage of spleen macrophages engulfing erythrocytes and neutrophils and the fraction of lung macrophages with ingested red cells (but not neutrophils, Figure 2A). In contrast, we found no differences in efferocytosis of spleen macrophages for AA mice treated with imatinib (Suppl. Figure 5S). Spleen macrophages from imatinib-treated SCD mice had significantly higher expression of phagocytic receptors CD68, CD206, Tim-4, and CD36, indicating that the imatinib-induced increase in efferocytosis is accompanied by a proresolutive macrophage phenotype (Figure 2B, Suppl. Figure 6S). Thus, imatinib beneficially modulates inflammatory response by inducing a pro-resolving profile of macrophages. These results also prompted us to test its action in target organs such as lung, kidney, and in known mediators of inflammatory response and resolution.

Imatinib reduces lung injury and modulates H/R-induced inflammatory response in SCD mice

In lung from imatinib-treated SCD mice exposed to H/R, we observed a significant reduction of inflammatory lung cell infiltrate within the alveolar walls as well as of edema when compared to vehicle-treated animals (Figure 3A; Table 1). Indeed, we found reduction of bronchoalveolar lavage total leukocyte and protein content in SCD mice treated with imatinib

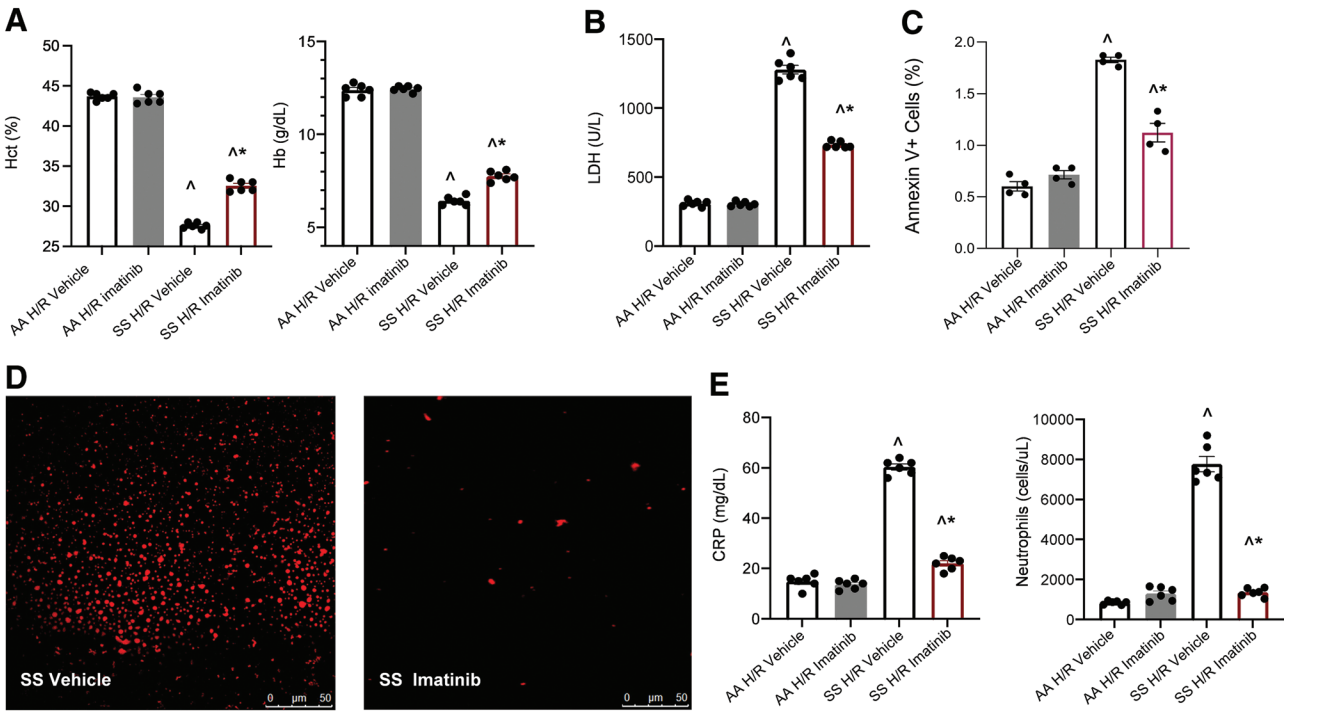

Figure 1. Imatinib improves red cell features and reduces inflammation in SCD mice. (A) Hct and Hb values in healthy (AA) and sickle (SS) mice exposed to H/R: hypoxia (8% oxygen; 10 h), followed by reoxygenation (21% oxygen; 3 h) treated with either vehicle or imatinib (50 mg/kg/d for 3 wk). Data are presented as mean ± SEM (n = 6; 3 female and 3 male mice). ^$P < 0.05$ compared with AA, *$P < 0.05$ compared with vehicle. (B) LDH plasma values in AA and SCD mice treated as in (A). Data are mean ± SEM (n = 6; 3 female and 3 male mice). ^$P < 0.05$ compared with AA, *$P < 0.05$ compared with vehicle. (C) Effect of imatinib on the amount of annexin V+ erythrocytes of AA and SCD mice treated as in (A). Data are presented as mean ± SEM (n = 4; 2 female and 2 male mice), ^$P < 0.05$ compared with AA, *$P < 0.05$ compared with vehicle. (D) Representative micropicture of erythroid microvesicles plasma from SCD mice exposed to H/R treated with either vehicle or imatinib. Erythroid vesicle quantification is shown in Suppl. Figure 2SB. (E) CRP plasma values (left panel) and peripheral neutrophils count (right panel) in AA and SCD mice treated as in (A). Data are mean ± SEM (n = 6; 3 female and 3 male mice). ^$P < 0.05$ compared with AA, *$P < 0.05$ compared with vehicle. CRP = C-reactive protein; H/R = hypoxia/reoxygenation stress; Hb = hemoglobin; Hct = hematocrit; LDH = lactate dehydrogenase; SCD = sickle cell disease; SEM = standard error of the mean.

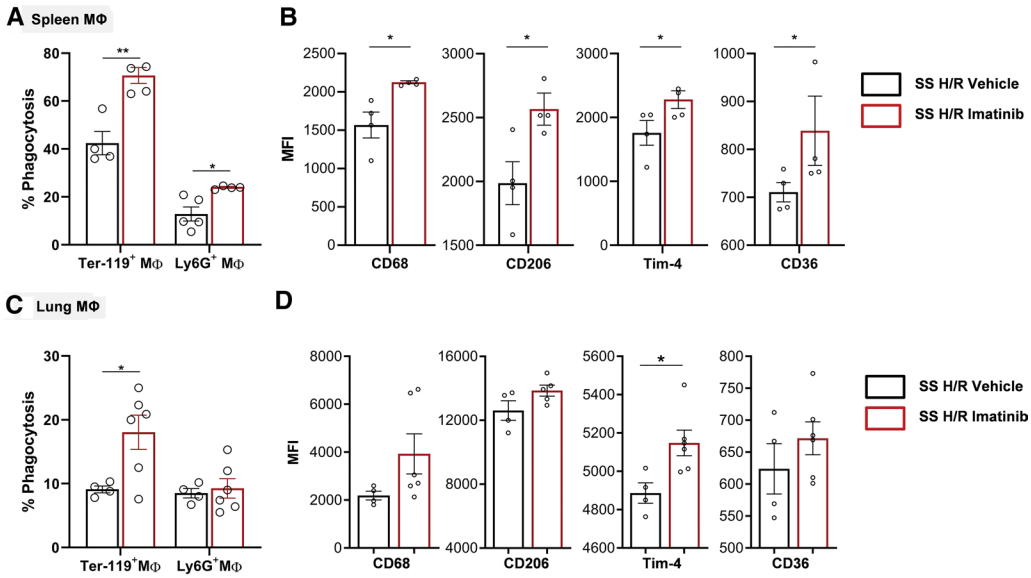

Figure 2. Imatinib enhances efferocytosis and a proresolutive phenotype of splenic and pulmonary macrophages in SCD mice. (A) In vivo splenic phagocytosis in SCD mice exposed to H/R: hypoxia (8% oxygen; 10 h), followed by reoxygenation (21% oxygen; 3 h) treated with either vehicle (n = 4–5 mice; 2 male/2 female; 2 male/3 female) or imatinib (n = 4 mice; 2 male/2 female) (50 mg/kg for 3 wk). Phagocytosis of erythrocytes and neutrophils were assessed, respectively, as the percentage of F4/80+/Ter-119+ and F4/80+/Ly6G+ double positive cells. Results are means ± SEM. (B) In vivo M1/M2 polarization of the splenic macrophages from SCD mice exposed to H/R treated with either vehicle or imatinib, determined by flow cytometric analysis using specific surface markers. Mean fluorescence intensities (MFI) of CD68, CD206, Tim-4, and CD36 in F4/80+ cells were analyzed. (C–D) As (A) and (B) in lung ((C) vehicle n = 4, 2 male/2 female, imatinib-treated mice, n = 6, 3 male/3 female; (D) CD68 and CD36: vehicle n = 4, 2 male/2 female; imatinib-treated mice, n = 6, 3 male/3 female; CD206 and Tim4: vehicle n = 4, 2 male/2 female, imatinib-treated mice, n = 5, 2 male/3 female). Data are mean ± SEM (n = 4–6; 2/3 female and 2/3 male mice). *$P < 0.05$ compared with vehicle. H/R = hypoxia/reoxygenation stress; SCD = sickle cell disease; SEM = standard error of the mean.

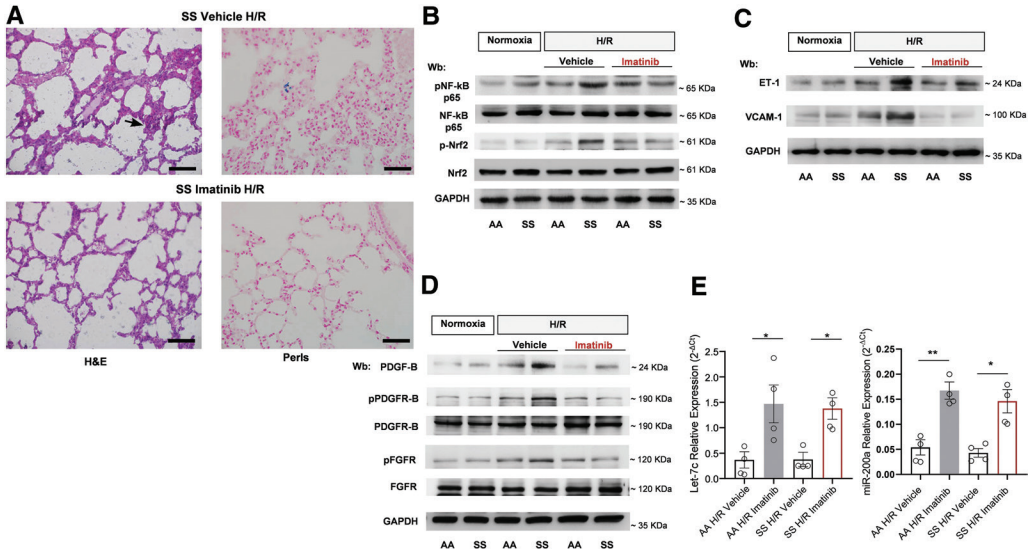

Figure 3. Imatinib beneficially modifies H/R-induced lung injury. (A) Representative micropicture of H&E-stained sections and Perls'-stained sections of lung at 200× magnification from SCD mice exposed to H/R: hypoxia (8% oxygen; 10 h), followed by reoxygenation (21% oxygen; 3 h) treated with either vehicle or imatinib (50 mg/kg/d for 3 wk) (scale bar: 50 μm) (see also Table 1). (B) Immunoblot analysis, using specific antibodies against phosphorylated (p)NF-κB p65, NF-κB p65, p-Nrf2, and Nrf2, in lung from healthy (AA) and SCD mice in normoxia and exposed to H/R treated with either vehicle or imatinib (2 female and 2 male mice). 75 μg/μL of protein loaded on an 8% T, 2.5%C polyacrylamide gel. GAPDH serves as protein loading control. One representative gel from 4 with similar results is shown. Densitometric analysis of immunoblots is shown in Suppl. Figure 6Sb. (C) Immunoblot analysis, using specific antibodies against ET-1 and VCAM-1 in lung from AA and SCD mice treated as in (B) (2 female and 2 male mice). 75 μg/μL of protein loaded on an 11% T, 2.5%C polyacrylamide gel. GAPDH serves as protein loading control. One representative gel from 4 with similar results is shown. Densitometric analysis of immunoblots is shown in Suppl. Figure 6Sc. (D) Immunoblot analysis, using specific antibodies against PDGF-B (75 μg/μL of protein loaded on an 11% T, 2.5%C polyacrylamide gel), phosphorylated (p-)PDGFR-B, PDGFR-B, p-FGFR, and FGFR in lung from AA and SCD mice treated as in (B) (2 female and 2 male mice). 75 μg/μL of protein loaded on an 8% T, 2.5%C polyacrylamide gel. GAPDH serves as protein loading control. One representative gel from 4 with similar results is shown. Densitometric analysis of immunoblots is shown in Suppl. Figure 6Se. (E) Expression of let-7c (left panel) and miR-200a (right panel), as determined using quantitative polymerase chain reaction, in the lungs of AA and SCD mice exposed to H/R treated with either vehicle or imatinib. Results are mean ± SEM from 4 mice each group (2 female and 2 male mice in each group). *$P < 0.05$ **$P < 0.01$. ET-1 = endothelin-1; H/R = hypoxia/reoxygenation stress; GAPDH = glyceraldehyde-3 phosphate dehydrogenase; H&E = hematoxylin and eosin; PDGF-B = platelet-derived growth factor-B; PDGFR-B = platelet-derived growth factor-receptor-B; p-FGFR = phospho-fibroblast growth factor receptor; SCD = sickle cell disease; SEM = standard error of the mean; SS = homozygous HbS; VCAM = vascular cell adhesion molecule-1.

Table 1

Effects of Imatinib on Lung and Kidney Pathology of Sickle Cell (SS) Mice Under Normoxia and Exposed to H/R Stress

	Normoxia	H/R	H/R Imatinib
Lung	**(n = 6)**	**(n = 6)**	**(n = 4)**
Inflammatory cell infiltrates	8.8 ± 0.7	96.8 ± 8.2[a]	15.4 ± 2.5[a,b]
Edema	0	+ (4/6) ++ (1/6)	0
Mucus	0	+ (1/6)	0
Kidney	(n = 6)	**(n = 6)**	**(n = 4)**
Inflammatory cell infiltrates	0	3.55 ± 0.46[a]	0.90 ± 0.013[a,b]
Necrosis	0	0	0

Lungs: *Mucus*: 0: no mucus, +: mucus filling <25% of the area of the bronchus circumference; ++ mucus filling 25%–50% of the area of the bronchus circumference; +++: 50%–100% of the area of the bronchus circumference at magnification of 400×. *Score for inflammatory cell infiltrate*: Quantification of inflammatory cell infiltrates was expressed as the mean of cells per field at magnification of 250×, as resulting by the analysis of at least 10 different fields on each hematoxylin-eosin–stained whole lung section (see also refs: [28] and [29]). Data are expressed as mean ± SEM. Kidney: *Score for inflammatory cell infiltrate*: Quantification of inflammatory cell infiltration in renal cortex of kidney was determined in hematoxylin-eosin–stained sections using a 0–4 scale based on the percentage of cell infiltrates occupied area in each filed. 0 (no sign of infiltration); 1 (1%–10% of the area with cell infiltration); 2 (11%–25%); 3 (26%–50%); 4 (50%). The mean of 15 randomly selected field were analyzed at magnification 400× (see also refs: [22] and [46]). Data are expressed as mean ± SEM. Statistical analysis: nonparametric pairwise Wilcoxon Rank Sum tests) was used; each group was balanced in sex (50% males–50% female). We repeated the comparisons for males and females separately with equivalent results; regarding the gender, our data did not show evidence of differences between males and females.

[a]$P < 0.05$ compared with normoxia.

[b]$P < 0.05$ compared with vehicle..

H/R = hypoxia/reoxygenation stress; SEM = standard error of the mean; SS = homozygous hemoglobin S.

compared with vehicle-treated animals exposed to H/R stress. This supports the beneficial effect of imatinib on H/R-induced abnormal pulmonary vascular leakage (Suppl. Figure 7Sa). Noteworthy, imatinib prevented the H/R-induced deposition of hemosiderin in macrophages, which are the only cells accumulating iron in lung.[10,46] Consistent with these observations, we found a significant decrease in the active forms of NF-kB p65 and Nrf2 induced by H/R in AA and SCD mice treated with imatinib (Figure 3B, Suppl. Figure 7Sc). We then evaluated key proinflammatory cytokines such as interleukin-6 (IL-6) and endothelin-1 (ET-1): their expression was significantly reduced in imatinib-treated mice exposed to H/R than in vehicle-treated groups (Figure 3C, Suppl. Figure 7Sb, 7Sd). With imatinib we also saw a reduction in the expression of heme-oxygenase-1 (a Nrf2-dependent antioxidant system involved in heme catabolism)[10,40] (Suppl. Figure 7Se). Noteworthy, imatinib prevented H/R-induced increase in expression of vascular adhesion molecule (VCAM-1) in lung from both AA and SCD mice exposed to H/R when compared with vehicle-treated animals (Figure 3C, Suppl. Figure 6Sd).

Imatinib has been shown to protect against both bleomycin acute lung injury and lung fibrosis by direct inhibition of both platelet-derived growth factor-receptor-B (PDGFR-B) and fibroblast growth factor-1 (FGF-R1).[47–49] We first evaluated the expression of PDGF-B, known to be a factor involved in lung extravascular matrix remodeling in response to hypoxia.[50,51] As shown in Figure 3D, imatinib prevented the H/R-induced increased expression of PDGF-B in both mouse models. This was accompanied by a reduction in activation of PDGFR-B and FGF-R1, both involved in modulation of extravascular matrix deposition and fibroblast activation (see also Suppl. Figure 7Sf).[52] In agreement, we found upregulation of miRNA Let-7c and miR-200a, both interfering with TGF-β1 mediate profibrotic pathways (Figure 3E).[10,53]

No sign of imatinib-related cardiotoxicity, assessed by heart ultrasonography, was found in SCD mice (Suppl. Figure 8Sa).[54] No evidence of liver toxicity by histopathologic analysis was detected in imatinib-treated SCD mice exposed to H/R when compared with vehicle-treated animals (Suppl. Figure 8Sb). Noteworthy, imatinib reduced inflammatory cell infiltrates in liver from SCD mice exposed to H/R (Suppl. Figure 8Sb).

These data provide in vivo evidence that imatinib treatment protects SCD mice against H/R-induced lung injury by suppressing key mediators of inflammation and vascular damage, modulating extravascular matrix remodeling.

Imatinib diminished H/R-induced kidney damage and modulates the local inflammatory response in SCD mice

We therefore examined if imatinib may protect SCD mice from H/R-induced kidney injury.[24] To avoid possible interfering factors related to either gender or age, we studied 4–6 month-old and gender-matched AA and SCD mice.[55,56] Treatment with imatinib significantly prevented the H/R-induced increase in creatinine and blood urea nitrogen plasma values in SCD mice compared with vehicle-treated SS animals (Figure 4A). Because the size of metabolic cage is not compatible with hypoxic chamber, we could not determine albuminuria in SCD mice exposed to H/R stress.

Histopathologic analysis of kidney from SCD mice exposed to H/R and treated with imatinib revealed a marked reduction in pericapillary and periglomerular inflammatory cell infiltration compared with vehicle-treated H/R animals (Figure 4B and Table 1). Reduction in inflammatory cell kidney infiltrates was also confirmed by flow-cytometry (Figure 4B, lower panel; Suppl. Figure 9S).

Perls' staining showed important iron deposits located in tubular epithelium, together with periglomerular capsule in vehicle-treated SCD mice exposed to H/R (Figure 4B). Iron deposition was markedly reduced in imatinib-treated SCD mice exposed to H/R, which were characterized by iron deposition mainly within the tubular epithelium (Figure 4B). This change may reflection diminished hemolysis (Figure 1B).

In kidneys from all imatinib-treated mice, we found a reduction in H/R-induced activation of NF-kB and Nrf2 (Figure 4C, Suppl. Figure 10Sa), a reduction in E-selectin and IL-1b expression (Suppl. Figure 10Sb) and a blunted expression of ET-1 and VCAM-1(Figure 4D, Suppl. Figure 10Sc).

Taken together, these data indicate that imatinib protects kidney against sickle cell–related H/R injury, modulating local inflammatory response and vascular activation.

Imatinib reduces the inflammatory-related profibrotic stimulus in kidney from SCD mice exposed to H/R stress

In kidney, H/R stress related to sickle cell VOCs represents a potent profibrotic stimulus,[57–60] which might be further amplified by the pro-oxidant effect of kidney iron deposition. We found increased protein oxidation in kidney of SCD mice exposed to H/R stress, which was significantly reduced by imatinib treatment (Suppl. Figure 11Sa). H/R stress and oxidation are both potent profibrotic stimuli for PDGF-B and PDGFR-B, which play a key role in mesangial cell proliferation and matrix accumulation in various kidney disease such as diabetic nephropathy.[24,61–63] As shown in Figure 5A, imatinib prevented H/R-induced increased expression of PDGF-B and activation of PDGFR-B (phospho-PDGFR-B form) in SCD mice exposed to H/R (Suppl. Figure 11Sb). The expression of miR-200a, previously shown to reduce renal fibrosis through the TGF-β1 system,[10,53,64] was increased in kidney from imatinib-treated AA and SCD mice, whereas the expression of let-7c was unaffected (Figure 5B). We also found a significant reduction of active TGF-β1 receptor in kidney from imatinib-treated AA and SCD mice (Figure 5C, Suppl. Figure 11Sc).

In different models of acute and chronic kidney injury, abnormalities in autophagy have been described.[65,66] These mainly involve the activation of mammalian target of rapamycin (mTOR), the gatekeeper of autophagy, with accumulation of

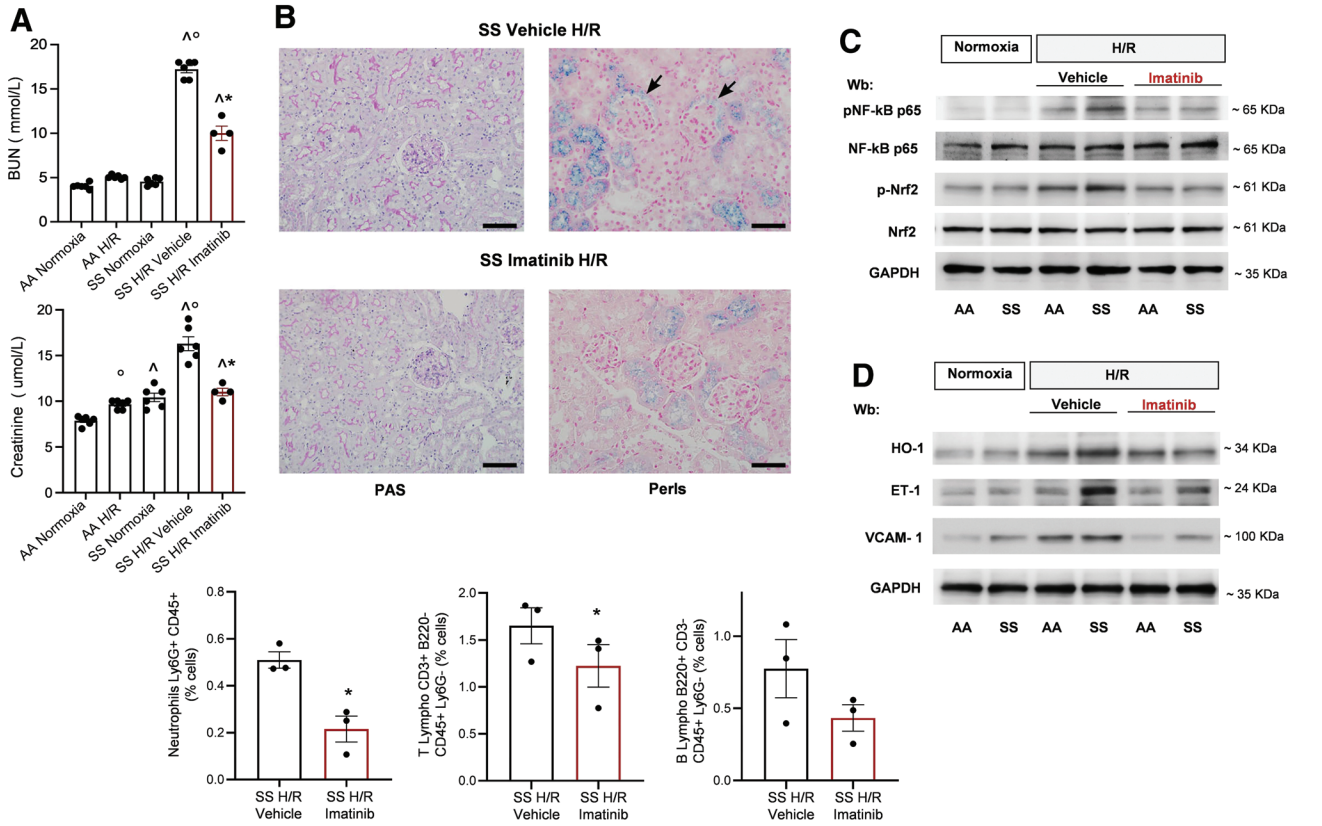

Figure 4. Imatinib reduces H/R-induced kidney damage modulating the local inflammatory response and the vascular activation. (A) BUN (upper panel) and plasma creatinine (lower panel) values in healthy (AA) and SCD mice under normoxia conditions or exposed to H/R: hypoxia (8% oxygen; 10 h), followed by reoxygenation (21% oxygen; 3 h) treated with either vehicle (n = 6; 3 female and 3 male mice) or imatinib (50 mg/kg/d for 3 wk) (n = 4; 2 female and 2 male mice). Data are means ± SEM. °$P < 0.05$ compared with normoxia, ^$P < 0.05$ compared with AA; *$P < 0.05$ compared with vehicle. (B) Upper panel: Representative PAS and Perls'-stained sections at 400× magnification. Black arrows: Iron deposits are located in tubular epithelium, together with periglomerular capsule (scale bar: 50 μm). Lower panel: Inflammatory cell infiltrates assessed by flow cytometric analysis of kidney tissue from SCD mice exposed to H/R treated with either vehicle or imatinib (n = 3 female mice). Data are means ± SEM (n = 3). *$P < 0.05$ compared with vehicle (see also Table 1). (C) Immunoblot analysis, using specific antibodies against phosphorylated (p-)NF-κB p65, NF-κB p65, p-Nrf2, and Nrf2, in kidney from AA and SCD mice in normoxia and exposed to H/R treated with vehicle or imatinib (2 female and 2 male mice). 75 μg/μL of protein loaded on an 8% T, 2.5%C polyacrylamide gel. GAPDH serves as protein loading control. One representative gel from 4 with similar results is shown. Densitometric analysis of immunoblots is shown in Suppl. Figure 9Sa. (D) Immunoblot analysis, using specific antibodies against HO-1 (40 μg/μL of protein loaded on an 11% T, 2.5%C polyacrylamide gel), ET-1 (75 μg/μL of protein loaded on an 11% T, 2.5%C polyacrylamide gel), and VCAM-1 (40 μg/μL of protein loaded on an 8% T, 2.5%C polyacrylamide gel) in lung from AA and SCD mice treated as in (C). GAPDH serves as protein loading control. One representative gel from 4 with similar results is shown. Densitometric analysis of immunoblots is shown in Suppl. Figure 9Sc. BUN = blood urea nitrogen; ET-1 = endothelin-1; GAPDH = glyceraldehyde-3 phosphate dehydrogenase; H/R = hypoxia/reoxygenation stress; HO-1 = heme-oxygenase-1; PAS = periodic acid-Schiff; SCD = sickle cell disease; SEM = standard error of the mean; VCAM-1 = vascular cell adhesion molecule-1.

p62, late phase autophagy marker.[65,66] mTOR is part of the signaling downstream of PDGFR.[65,66] Here, we found that imatinib treatment inhibited mTOR in kidney from both AA and SCD mice exposed to H/R stress when compared with vehicle-treated animals (Figure 5D, Suppl. Figure 11Sd). This was associated with significant reduction in H/R-induced activation of LC3 and accumulation of p62, indicating that the impaired autophagy in the vehicle-treated mice was ameliorated by imatinib treatment (Figure 5E, Suppl. Figure 11Se). An imatinib-induced reduction in accumulation of ubiquitinated proteins in kidney from SCD mice exposed to H/R was also found (Suppl. Figure 12S).

Thus, imatinib reduces H/R-induced profibrotic stimulus and may protect from progression of sickle cell–related kidney injury.

Imatinib protects against inflammatory vasculopathy during acute hypoxia/reoxygenation stress in SCD mice

In SCD, amplified inflammatory response and defective proresolving mechanisms result in endothelial dysfunction and vascular vulnerability leading to an inflammatory vasculopathy which plays a key role in acute organ damage.[8,9,67] Previous studies have shown that imatinib might beneficially impact inflammatory vasculopathy such as atherosclerosis.[23,68–70] Here, we found that imatinib significantly reduces the expression of VCAM-1 in aorta from SCD mice when compared with vehicle-treated animals, as determined by complementary approaches: in vivo molecular imaging MRI using VCAM-1–targeted Gd-based micelles and immunoblot analysis with specific anti-VCAM-1 antibody (Figure 6A, Suppl. Figure 13Sa). We also demonstrated a significant correlation between the aorta T_1-MRI contrast enhancement related to VCAM-1–targeted micelles and VCAM-1 detected by immunoblot analysis on isolated aorta for the same mice analyzed by imaging (Suppl. Figure 13Sa, lower panel). Imatinib prevented the H/R-induced upregulation of markers of inflammatory vasculopathy such as VCAM-1, E-Selectin, and ET-1 (Figure 6B, Suppl. Figure 13Sb). In agreement, imatinib prevented the H/R-induced overactivation of PDGFR-B in isolated aorta of SCD mice when compared with vehicle-treated animals (Figure 6C, Suppl. Figure 13Sc). These data indicate that imatinib prevents severe vascular dysfunction and disease progression in SCD exposed to H/R stress, mimicking sickle cell–related VOCs.

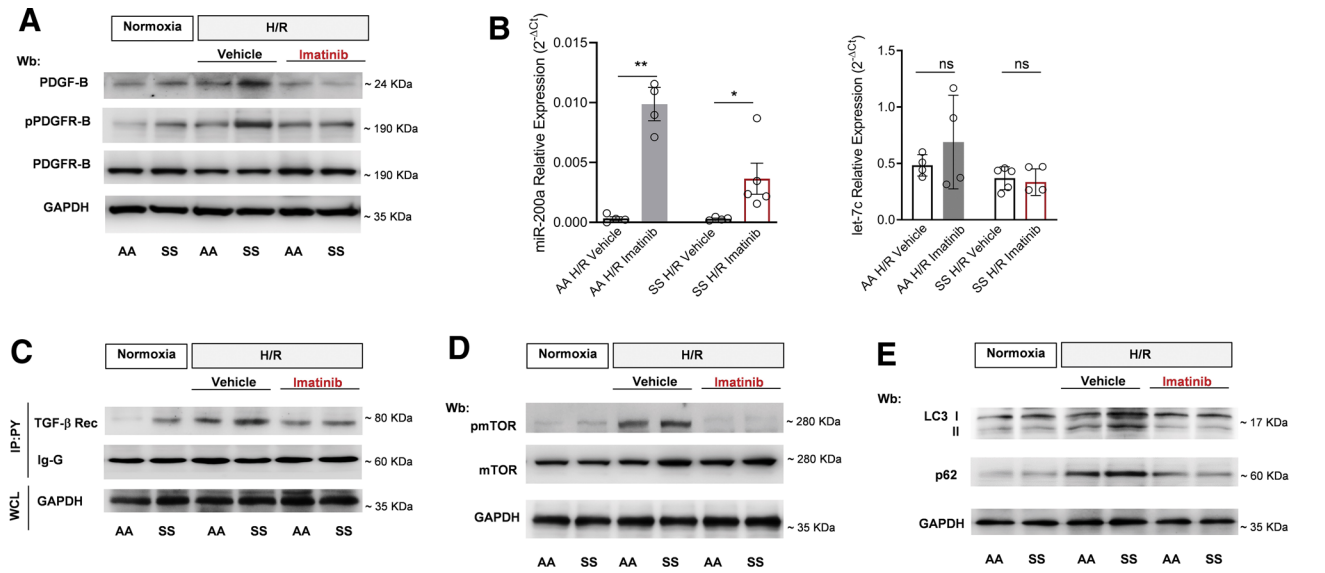

Figure 5. Imatinib reduces inflammatory related profibrotic stimulus and modulates autophagy in kidney of SCD mice. (A) Immunoblot analysis, using specific antibodies against PDGF-B (75 µg/µL of protein loaded on an 11% T, 2.5%C polyacrylamide gel), phosphorylated (p-)PDGFR-B, PDGFR-B, in kidney from healthy (AA) and SCD mice under normoxia conditions or exposed to H/R: hypoxia (8% oxygen; 10 h), followed by reoxygenation (21% oxygen; 3 h) treated with either vehicle or imatinib (50 mg/kg daily for 3 wk). 75 µg/µL of protein loaded on an 8% T, 2.5%C polyacrylamide gel. One representative gel from 3 with similar results is shown. Densitometric analysis of immunoblots is shown in Suppl. Figure 10Sb. (B) Expression of miR-200a (left panel) and let-7c (right panel), as determined using quantitative polymerase chain reaction, in kidney of AA (n = 4, 2 female/2 male) and SCD (miR-200a SS H/R vehicle n = 4, 2 female/2 male; SS H/R imatinib n = 5, 2 male/3 female; let7c SS H/R vehicle n = 5, 2 female/3 male; SS H/R imatinib n = 4, 2 male/2 female) mice exposed to H/R and treated with either vehicle or imatinib. Results are shown as mean ± SEM from 3 to 5 mice per group. $^{*}P < 0.05$ $^{**}P < 0.01$. (C) Kidney immunoprecipitation using specific antiphosphotyrosine antibodies (IP: pY), revealed with specific anti-TGF receptor (Rec) antibody (75 µg/µL of protein loaded on an 8% T, 2.5%C polyacrylamide gel). GAPDH in WCL and Ig-G are used as loading controls. One representative gel from 3 others with similar results is presented. Densitometric analysis of immunoblots is shown in Suppl. Figure 10Sc. (D) Immunoblot analysis, using specific antibodies against phosphorylated (p-)mTOR and mTOR in kidney from AA and SCD mice treated as in (A) (2 female and 2 male mice). 100 µg/µL of protein loaded on an 8% T, 2.5%C polyacrylamide gel. One representative gel from 4 with similar results is shown. Densitometric analysis of immunoblots is shown in Suppl. Figure 10Sd. (E) Immunoblot analysis, using specific antibodies against LC3 I/II (75 µg/µL of protein loaded on an 14% T, 2.5%C polyacrylamide gel) and p62 (50 µg/µL of protein loaded on an 8% T, 2.5%C polyacrylamide gel) in kidney from AA and SCD mice treated as in a (2 female and 2 male mice). One representative gel from 4 with similar results is shown. Densitometric analysis of immunoblots is shown in Suppl. Figure 10Se. GAPDH = glyceraldehyde-3 phosphate dehydrogenase; H/R = hypoxia/reoxygenation stress; mTOR = mammalian target of rapamycin; PDGF-B = platelet-derived growth factor-B; PDGFR-B = platelet-derived growth factor-receptor-B; SCD = sickle cell disease; SEM = standard error of the mean; TGF = transforming growth factor; WCL = whole-cell lysate.

DISCUSSION

The present study, in a widely used and validated mouse model for SCD, provides multiple lines of evidence supporting beneficial effects of imatinib in anemia and acute and chronic organ damage in SCD. These new data further support the prior in vitro data and the case reports in SCD patient treated with imatinib due to concomitant CML, which have suggested that imatinib therapy could be a disease modifier in SCD. Our in vivo data in the SCD mouse model provide evidence for multiple effects of imatinib on crucial signal transduction pathways involved in the pathogenesis of sickle cell–related organ damage.

In SCD, imatinib targets proinflammatory and profibrotic response to ischemic reperfusion damage. Indeed, imatinib lowered both systemic and local proinflammatory responses, most-likely by immunomodulatory effects on both neutrophils and organ macrophages (Figure 6D). Moreover, the proresolving profile of macrophages found in both lung and spleen of imatinib-treated animals optimizes phagocytosis and provides an additional mechanism of action of imatinib in accelerating the proresolving events in SCD. This is further corroborated by the reduction in the activation of NF-kB with downregulation of IL-6 and ET-1 expression in lung and kidney from imatinib-treated SCD mice exposed to H/R stress when compared with vehicle-treated animals. The protective effect of imatinib against inflammatory vasculopathy is also supported by the reduction of VCAM-1 expression in lung, kidney, and isolated aorta induced by H/R, as determined by different methodologic approaches (Figure 6D). This agrees with the observation that imatinib prevented ex vivo neutrophil adhesion to TNF-α–activated vascular endothelial cells.

Recently, we show that H/R stress mimicking acute sickle cell–related VOC promotes lung extracellular matrix remodeling and the activation of profibrogenic pathways such as PDGF-B.[10,71] Imatinib has been also reported to specifically target the PDGF-B signaling pathway reducing lung fibrosis.[49,72] In SCD mice exposed to H/R stress, imatinib prevented the H/R-induced activation of receptors for either PDGF-B or FGF, involved in progression of lung fibrosis. This was associated with the upregulation of let-7c and miR-200a, interfering with TGF-b1 mediate profibrotic pathways.[10,53] The antifibrotic effect of imatinib, as reduced activation of both PGF-B and TGF-β1 receptors, was also observed in kidney from imatinib-treated SCD mice exposed to H/R stress (Figure 6D). This agrees with previous reports in other models of kidney disease showing that inhibition or silencing of PDGF-B pathway leads to reduction in extracellular matrix remodeling and cell oxidation.[63,66,73,74] Indeed, in bosutinib-treated SCD mice, no major change in hematologic phenotype as well as in H/R-induced increased VCAM-1 expression and overactivation of PDGF-R were observed (Suppl. Figure 14Sa–d).

Finally, in imatinib-treated SCD mice, we found decreased oxidation of kidney proteins. In combination with the inhibition of PDGFR-B that is upstream in signaling pathway of mTOR, this results in inhibition of mTOR and activation of autophagy.

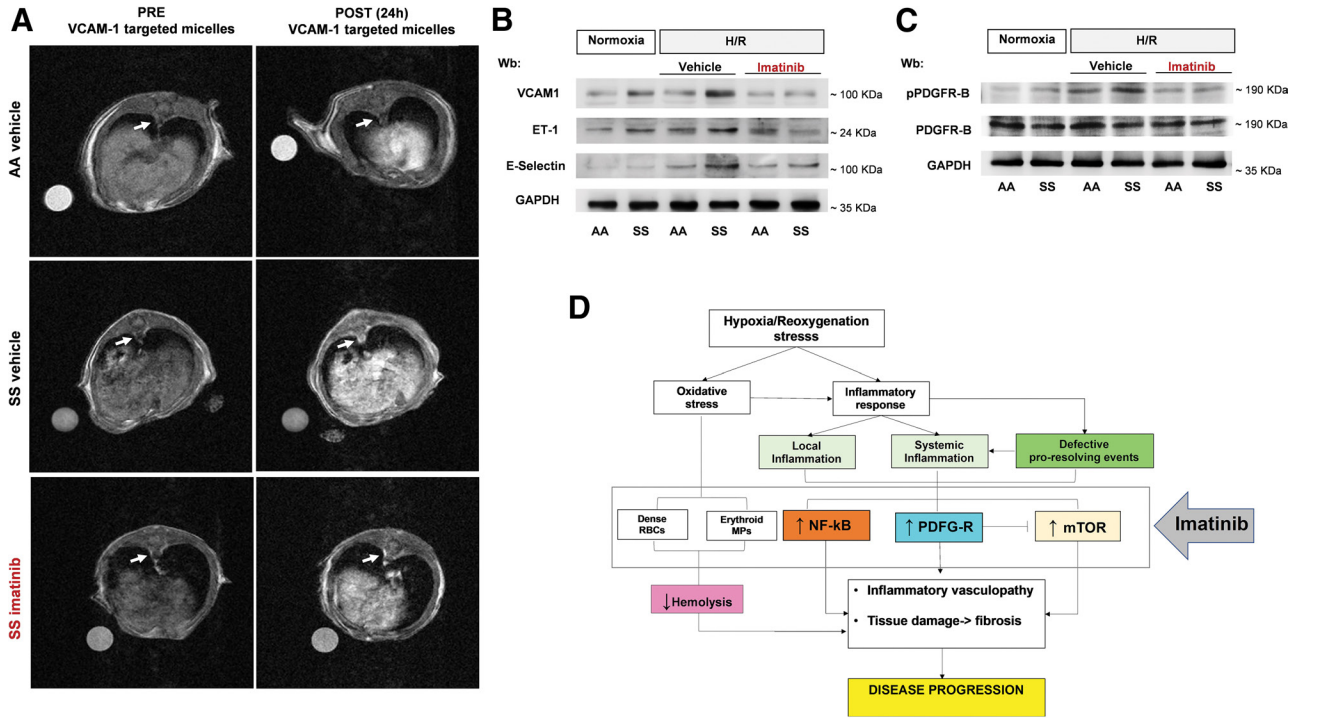

Figure 6. Imatinib protects SCD mice against inflammatory vasculopathy during H/R stress. (A) Representative T1-weighted axial images of the abdominal aorta acquired before (PRE) and 24 h (POST) the injection of VCAM-1–targeted micelles in healthy (AA) vehicle, HbS homozygous (SS) vehicle, or SS imatinib-treated mice. The white arrows indicate the abdominal aorta sections. (B) Immunoblot analysis, using specific antibodies against VCAM-1 (40 μg/μL of protein loaded on an 8% T, 2.5%C polyacrylamide gel), ET-1 (75 μg/μL of protein loaded on an 11% T, 2.5%C polyacrylamide gel), and E-selectin (75 μg/μL of protein loaded on an 8% T, 2.5%C polyacrylamide gel) in isolated aorta from AA and SCD mice under normoxia or exposed to H/R treated with either vehicle or imatinib (2 female and 2 male mice). One representative gel from 4 with similar results is shown. Densitometric analysis of immunoblots is shown in Suppl. Figure 12Sb. (C) Immunoblot analysis, using specific antibodies against phosphorylated (p-)PDGFR-B and PDGFR-B in isolated aorta from AA and SCD mice treated as in a (2 female and 2 male mice). 75 μg/μL of protein loaded on an 8% T, 2.5%C polyacrylamide gel. One representative gel from 4 with similar results is shown. Densitometric analysis of immunoblots is shown in Suppl. Figure 12Sc. (D) Schematic diagram of multimodal action of imatinib in humanized mouse model for SCD. Imatinib improves red cell features with the reduction H/R-induced hemolysis and generation of erythroid microvesicles. This is combined with modulation of local inflammatory response with modulation of NF-kB–dependent response and inhibition of profibrotic PDGF-B/TGF-β signaling pathway. This protects against severe H/R-mediated cell injury with improvement of autophagy, ensuring cell survival against H/R stress. Collectively imatinib protects against H/R stress, mimicking acute sickle cell–related vaso-occlusive crisis, modulating local and systemic inflammatory response, and preventing disease progression. ET-1 = endothelin-1; H/R = hypoxia/reoxygenation stress; NF-kB = nuclear factor-kB; PDGF-B = platelet-derived growth factor-B; PDGFR-B = platelet-derived growth factor-receptor-B; SCD = sickle cell disease; TGF-b = transforming growth factor-b; VCAM-1 = vascular cell adhesion molecule-1.

Indeed, we found (i) reduction of LC3 I/II, an autophagy initiator; (ii) decreased accumulation of p62, a late phase autophagy cargo protein; and (iii) reduced accumulation of ubiquinated proteins. These data point to an improvement of autophagic flux in kidney from imatinib-treated SCD mice exposed to H/R (Figure 6D). An efficient autophagy is crucial to ensure the clearance of damage proteins, whose accumulation promotes cell oxidation redirecting cells toward apoptosis and progression of kidney damage.[66,73–75]

In conclusion, imatinib protects against H/R-induced organ damage in humanized SCD and improves multiple key points of its disease pathophysiology, resembling the multimodal action of HU. The recent development of new therapeutic options such as voxelotor, an oral anti-sickling agent, or crizanlizumab, a monoclonal anti-P-Selectin antibody, has opened a new era for clinical management of patients with SCD. Our data generate a rational for considering imatinib to treat SCD. Imatinib has already been tested in clinical trials and used for 2 decades in CML patients. This is extremely helpful in design the follow-up strategy to early intersect possible adverse events related to long-term treatment with imatinib in SCD. Here, we have excluded a worsening of cardiac function in humanized SCD mice treated with imatinib and the literature shows that patients with SCD and CML have well-tolerated imatinib treatment without severe adverse events.[14–16]

Collectively, our data may substantially reduce R&D costs and provide an accelerated pipeline of clinical studies as this potentially new therapeutic option for SCD. Last but not least, our study validates VCAM-1 MRI as a new in vivo technique to be combined with already available prognostic markers (or diagnostic techniques) for monitoring inflammatory vasculopathy in patients with SCD.

ACKNOWLEDGMENTS

The authors thank Dr. Barbara Gianesin, FOR ANEMIA foundation for statistical consultancy.

AUTHOR CONTRIBUTIONS

EF, AM, AR designed, performed experiments, and contributed to paper writing. FG, ET carried out imaging RNM analysis, analyzed data, and contributed to paper writing. AG, MD carried out heart ultrasonography, analyzed data, and contributed to paper writing. ENW and MM carried out in vitro adhesion experiments and analyzed data. CL and AJ carried out histopathologic analyses, analyzed data. FT and AP carried out erythroid microvesicles studies, analyzed data, and contributed to paper writing. RR, AI, DM carried out RT-PCR analyses, analyzed data, and contributed to paper writing. AA performed HPLC M/MS analyses and generated data on imatinib liver concentration. II, VR, RP, AS analyzed data. CB and LDF designed the study, analyzed data, and wrote the paper.

DISCLOSURES

CB has a consulting agreement with Pfizer on sickle cell disease. All the other authors have no conflicts of interest to disclose.

SOURCES OF FUNDING

This work was supported by FUR-UNIVR (LDF).

REFERENCES

1. Noomuna P, Risinger M, Zhou S, et al. Inhibition of Band 3 tyrosine phosphorylation: a new mechanism for treatment of sickle cell disease. *Br J Haematol*. 2020;190:599–609.
2. Cannon M, Phillips H, Smith S, et al. Large-scale drug screen identifies FDA-approved drugs for repurposing in sickle-cell disease. *J Clin Med*. 2020;9:2276.
3. Pushpakom S, Iorio F, Eyers PA, et al. Drug repurposing: progress, challenges and recommendations. *Nat Rev Drug Discov*. 2019;18:41–58.
4. Gardner K, Douiri A, Drasar E, et al. Survival in adults with sickle cell disease in a high-income setting. *Blood*. 2016;128:1436–1438.
5. Platt OS, Brambilla DJ, Rosse WF, et al. Mortality in sickle cell disease. Life expectancy and risk factors for early death. *N Engl J Med*. 1994;330:1639–1644.
6. Powars DR, Chan LS, Hiti A, et al. Outcome of sickle cell anemia: a 4-decade observational study of 1056 patients. *Medicine (Baltim)*. 2005;84:363–376.
7. Maitra P, Caughey M, Robinson L, et al. Risk factors for mortality in adult patients with sickle cell disease: a meta-analysis of studies in North America and Europe. *Haematologica*. 2017;102:626–636.
8. Matte A, Cappellini MD, Iolascon A, et al. Emerging drugs in randomized controlled trials for sickle cell disease: are we on the brink of a new era in research and treatment? *Expert Opin Investig Drugs*. 2020;29:23–31.
9. De Franceschi L, Cappellini MD, Olivieri O. Thrombosis and sickle cell disease. *Semin Thromb Hemost*. 2011;37:226–236.
10. Matte A, Recchiuti A, Federti E, et al. Resolution of sickle cell disease-associated inflammation and tissue damage with 17 R-resolvin D1. *Blood*. 2019;133:252–265.
11. Howard J, Ataga KI, Brown RC, et al. Voxelotor in adolescents and adults with sickle cell disease (HOPE): long-term follow-up results of an international, randomised, double-blind, placebo-controlled, phase 3 trial. *Lancet Haematol*. 2021;8:e323–e333.
12. Vichinsky E, Hoppe CC, Ataga KI, et al. A phase 3 randomized trial of voxelotor in sickle cell disease. *N Engl J Med*. 2019;381:509–519.
13. Ataga KI, Kutlar A, Kanter J, et al. Crizanlizumab for the prevention of pain crises in sickle cell disease. *N Engl J Med*. 2017;376:429–439.
14. Murphy M, Close J, Lottenberg R, et al. Effectiveness of imatinib therapy for sickle cell anemia and chronic myeloid leukemia. *Am J Med Sci*. 2014;347:254–255.
15. Close J, Lottenberg R. Effectiveness of imatinib therapy for a patient with sickle cell anemia and chronic myelocytic leukemia. *Blood*. 2009;114:2559.
16. Stankovic Stojanovic K, Thioliere B, Garandeau E, et al. Chronic myeloid leukaemia and sickle cell disease: could imatinib prevent vaso-occlusive crisis? *Br J Haematol*. 2011;155:271–272.
17. Vincent L, Vang D, Nguyen J, et al. Mast cell activation contributes to sickle cell pathobiology and pain in mice. *Blood*. 2013;122:1853–1862.
18. Kutlar A. GLEE-ful for sickle cell pain? *Blood*. 2013;122:1846–1847.
19. Tran H, Mittal A, Sagi V, et al. Mast cells induce blood brain barrier damage in SCD by causing endoplasmic reticulum stress in the endothelium. *Front Cell Neurosci*. 2019;13:56.
20. Wolf AM, Wolf D, Rumpold H, et al. The kinase inhibitor imatinib mesylate inhibits TNF-{alpha} production in vitro and prevents TNF-dependent acute hepatic inflammation. *Proc Natl Acad Sci U S A*. 2005;102:13622–13627.
21. Buchdunger E, O'Reilly T, Wood J. Pharmacology of imatinib (STI571). *Eur J Cancer*. 2002;38(suppl 5):S28–S36.
22. Liang S, Yu H, Chen X, et al. PDGF-BB/KLF4/VEGF signaling axis in pulmonary artery endothelial cell angiogenesis. *Cell Physiol Biochem*. 2017;41:2333–2349.
23. Lassila M, Allen TJ, Cao Z, et al. Imatinib attenuates diabetes-associated atherosclerosis. *Arterioscler Thromb Vasc Biol*. 2004;24:935–942.
24. Lassila M, Jandeleit-Dahm K, Seah KK, et al. Imatinib attenuates diabetic nephropathy in apolipoprotein E-knockout mice. *J Am Soc Nephrol*. 2005;16:363–373.
25. Pichavaram P, Shawky NM, Hartney TJ, et al. Imatinib improves insulin resistance and inhibits injury-induced neointimal hyperplasia in high fat diet-fed mice. *Eur J Pharmacol*. 2021;890:173666.
26. Maihofer NA, Suleiman S, Dreymuller D, et al. Imatinib relaxes the pulmonary venous bed of guinea pigs. *Respir Res*. 2017;18:32.
27. Zitvogel L, Rusakiewicz S, Routy B, et al. Immunological off-target effects of imatinib. *Nat Rev Clin Oncol*. 2016;13:431–446.
28. Kalish BT, Matte A, Andolfo I, et al. Dietary ω-3 fatty acids protect against vasculopathy in a transgenic mouse model of sickle cell disease. *Haematologica*. 2015;100:870–880.
29. Matte A, Federti E, Winter M, et al. Bitopertin, a selective oral GLYT1 inhibitor, improves anemia in a mouse model of β-thalassemia. *JCI Insight*. 2019;4:e130111.
30. Matte A, Low PS, Turrini F, et al. Peroxiredoxin-2 expression is increased in beta-thalassemic mouse red cells but is displaced from the membrane as a marker of oxidative stress. *Free Radic Biol Med*. 2010;49:457–466.
31. Brugnara C, Armsby CC, De Franceschi L, et al. Ca(2+)-activated K+ channels of human and rabbit erythrocytes display distinctive patterns of inhibition by venom peptide toxins. *J Membr Biol*. 1995;147:71–82.
32. Matte A, Federti E, Kung C, et al. The pyruvate kinase activator mitapivat reduces hemolysis and improves anemia in a beta-thalassemia mouse model. *J Clin Invest*. 2021;131:e144206.
33. Matte A, De Falco L, Iolascon A, et al. The interplay between peroxiredoxin-2 and nuclear factor-erythroid 2 is important in limiting oxidative mediated dysfunction in beta-thalassemic erythropoiesis. *Antioxid Redox Signal*. 2015;23:1284–1297.
34. Brugnara C, de Franceschi L. Effect of cell age and phenylhydrazine on the cation transport properties of rabbit erythrocytes. *J Cell Physiol*. 1993;154:271–280.
35. de Franceschi L, Turrini F, Honczarenko M, et al. In vivo reduction of erythrocyte oxidant stress in a murine model of beta-thalassemia. *Haematologica*. 2004;89:1287–1298.
36. Wolf A, Couttet P, Dong M, et al. Imatinib does not induce cardiotoxicity at clinically relevant concentrations in preclinical studies. *Leuk Res*. 2010;34:1180–1188.
37. Puttini M, Coluccia AM, Boschelli F, et al. In vitro and in vivo activity of SKI-606, a novel Src-Abl inhibitor, against imatinib-resistant Bcr-Abl+ neoplastic cells. *Cancer Res*. 2006;66:11314–11322.
38. Matte A, De Falco L, Federti E, et al. Peroxiredoxin-2: a novel regulator of iron homeostasis in ineffective erythropoiesis. *Antioxid Redox Signal*. 2018;28:1–14.
39. De Franceschi L, Bertoldi M, Matte A, et al. Oxidative stress and beta-thalassemic erythroid cells behind the molecular defect. *Oxid Med Cell Longev*. 2013;2013:985210.
40. Federti E, Matté A, Ghigo A, et al. Peroxiredoxin-2 plays a pivotal role as multimodal cytoprotector in the early phase of pulmonary hypertension. *Free Radic Biol Med*. 2017;112:376–386.
41. Pagoto A, Stefania R, Garello F, et al. Paramagnetic phospholipid-based micelles targeting VCAM-1 receptors for MRI visualization of inflammation. *Bioconjug Chem*. 2016;27:1921–1930.
42. Guo J, Guan Q, Liu X, et al. Relationship of clusterin with renal inflammation and fibrosis after the recovery phase of ischemia-reperfusion injury. *BMC Nephrol*. 2016;17:133–148.
43. Schwarz M, Taubitz A, Eltrich N, et al. Analysis of TNF-mediated recruitment and activation of glomerular dendritic cells in mouse kidneys by compartment-specific flow cytometry. *Basic Res*. 2013;84:116–129.
44. Dalle Carbonare L, Matte A, Valenti MT, et al. Hypoxia-reperfusion affects osteogenic lineage and promotes sickle cell bone disease. *Blood*. 2015;126:2320–2328.
45. Nguyen J, Abdulla F, Chen C, et al. Phenotypic characterization the twones sickle mice. *Blood*. 2014;124:4916.
46. Woodfin A, Beyrau M, Voisin MB, et al. ICAM-1-expressing neutrophils exhibit enhanced effector functions in murine models of endotoxemia. *Blood*. 2016;127:898–907.
47. Daniels CE, Wilkes MC, Edens M, et al. Imatinib mesylate inhibits the profibrogenic activity of TGF-beta and prevents bleomycin-mediated lung fibrosis. *J Clin Invest*. 2004;114:1308–1316.
48. Rhee CK, Lee SH, Yoon HK, et al. Effect of nilotinib on bleomycin-induced acute lung injury and pulmonary fibrosis in mice. *Respiration*. 2011;82:273–287.
49. Iqbal N, Iqbal N. Imatinib: a breakthrough of targeted therapy in cancer. *Chemother Res Pract*. 2014;2014:357027.
50. Schermuly RT, Dony E, Ghofrani HA, et al. Reversal of experimental pulmonary hypertension by PDGF inhibition. *J Clin Invest*. 2005;115:2811–2821.

51. Salabei JK, Cummins TD, Singh M, et al. PDGF-mediated autophagy regulates vascular smooth muscle cell phenotype and resistance to oxidative stress. *Biochem J*. 2013;451:375–388.
52. MacKenzie B, Korfei M, Henneke I, et al. Increased FGF1-FGFRc expression in idiopathic pulmonary fibrosis. *Respir Res*. 2015;16:83.
53. Yang S, Banerjee S, de Freitas A, et al. Participation of miR-200 in pulmonary fibrosis. *Am J Pathol*. 2012;180:484–493.
54. Ribeiro AL, Marcolino MS, Bittencourt HN, et al. An evaluation of the cardiotoxicity of imatinib mesylate. *Leuk Res*. 2008;32:1809–1814.
55. Kasztan M, Fox BM, Lebensburger JD, et al. Hyperfiltration predicts long-term renal outcomes in humanized sickle cell mice. *Blood Adv*. 2019;3:1460–1475.
56. Kasztan M, Aban I, Hande SP, et al. Sex differences in the trajectory of glomerular filtration rate in pediatric and murine sickle cell anemia. *Blood Adv*. 2020;4:263–265.
57. Deux JF, Audard V, Brugieres P, et al. Magnetic resonance imaging assessment of kidney oxygenation and perfusion during sickle cell vaso-occlusive crises. *Am J Kidney Dis*. 2017;69:51–59.
58. Schein A, Enriquez C, Coates TD, et al. Magnetic resonance detection of kidney iron deposition in sickle cell disease: a marker of chronic hemolysis. *J Magn Reson Imaging*. 2008;28:698–704.
59. Sharpe CC, Thein SL. How I treat renal complications in sickle cell disease. *Blood*. 2014;123:3720–3726.
60. Saraf SL, Zhang X, Kanias T, et al. Haemoglobinuria is associated with chronic kidney disease and its progression in patients with sickle cell anaemia. *Br J Haematol*. 2014;164:729–739.
61. Heldin CH, Westermark B. Mechanism of action and in vivo role of platelet-derived growth factor. *Physiol Rev*. 1999;79:1283–1316.
62. Alan S, Salva E, Yilmaz I, et al. The effectiveness of chitosan-mediated silencing of PDGF-B and PDGFR-beta in the mesangial proliferative glomerulonephritis therapy. *Exp Mol Pathol*. 2019;110:104280.
63. Uehara G, Suzuki D, Toyoda M, et al. Glomerular expression of platelet-derived growth factor (PDGF)-A, -B chain and PDGF receptor-alpha, -beta in human diabetic nephropathy. *Clin Exp Nephrol*. 2004;8:36–42.
64. Brennan EP, Nolan KA, Borgeson E, et al. Lipoxins attenuate renal fibrosis by inducing let-7c and suppressing TGFbetaR1. *J Am Soc Nephrol*. 2013;24:627–637.
65. Grahammer F, Haenisch N, Steinhardt F, et al. mTORC1 maintains renal tubular homeostasis and is essential in response to ischemic stress. *Proc Natl Acad Sci U S A*. 2014;111:E2817–E2826.
66. Kaushal GP, Chandrashekar K, Juncos LA, et al. Autophagy function and regulation in kidney disease. *Biomolecules*. 2020;10:100.
67. Manwani D, Frenette PS. Vaso-occlusion in sickle cell disease: pathophysiology and novel targeted therapies. *Blood*. 2013;122:3892–3898.
68. Ostman A, Heldin CH. Involvement of platelet-derived growth factor in disease: development of specific antagonists. *Adv Cancer Res*. 2001;80:1–38.
69. Prilepskii AY, Serov NS, Kladko DV, et al. Nanoparticle-based approaches towards the treatment of atherosclerosis. *Pharmaceutics*. 2020;12:1056.
70. Vorkapic E, Dugic E, Vikingsson S, et al. Imatinib treatment attenuates growth and inflammation of angiotensin II induced abdominal aortic aneurysm. *Atherosclerosis*. 2016;249:101–109.
71. Perros F, Montani D, Dorfmuller P, et al. Platelet-derived growth factor expression and function in idiopathic pulmonary arterial hypertension. *Am J Respir Crit Care Med*. 2008;178:81–88.
72. Aono Y, Kishi M, Yokota Y, et al. Role of platelet-derived growth factor/platelet-derived growth factor receptor axis in the trafficking of circulating fibrocytes in pulmonary fibrosis. *Am J Respir Cell Mol Biol*. 2014;51:793–801.
73. Dolman ME, van Dorenmalen KM, Pieters EH, et al. Imatinib-ULS-lysozyme: a proximal tubular cell-targeted conjugate of imatinib for the treatment of renal diseases. *J Control Release*. 2012;157:461–468.
74. Baumann M, Leineweber K, Tewiele M, et al. Imatinib ameliorates fibrosis in uraemic cardiac disease in BALB/c without improving cardiac function. *Nephrol Dial Transplant*. 2010;25:1817–1824.
75. Lee JY, Chang JW, Yang WS, et al. Albumin-induced epithelial-mesenchymal transition and ER stress are regulated through a common ROS-c-Src kinase-mTOR pathway: effect of imatinib mesylate. *Am J Physiol Renal Physiol*. 2011;300:F1214–F1222.